L. MIHALCEANU,[1] D.A. BOZHKO,[1, 2] V.I. VASYUCHKA,[1] A.A. SERGA,[1]
B. HILLEBRANDS,[1] A. POMYALOV,[3] V.S. L'VOV,[3] V.S. TYBERKEVYCH[4]

[1] Fachbereich Physik and Landesforschungszentrum OPTIMAS,
  Technische Universität Kaiserslautern
  (67663 Kaiserslautern, Germany; e-mail: mihalcea@rhrk.uni-kl.de)

[2] James Watt School of Engineering, University of Glasgow
  (Glasgow G12 8LT, United Kingdom; e-mail: dbozhko@uccs.edu)

[3] Department of Chemical and Biological Physics, Weizmann Institute of Science
  (Rehovot 76100, Israel; e-mail: Anna.Pomyalov@weizmann.ac.il)

[4] Department of Physics, Oakland University
  (Rochester MI 48309, United States; e-mail: tyberkev@oakland.edu)

MAGNON BOSE–EINSTEIN CONDENSATE AND SUPERCURRENTS OVER A WIDE TEMPERATURE RANGE

Magnon Bose–Einstein Condensates (BECs) and supercurrents are coherent quantum phenomena, which appear on a macroscopic scale in parametrically populated solid state spin systems. One of the most fascinating and attractive features of these processes is the possibility of magnon condensation and supercurrent excitation even at room temperature. At the same time, valuable information about a magnon BEC state, such as its lifetime, its formation threshold, and coherence, is provided by experiments at various temperatures. Here, we use Brillouin Light Scattering (BLS) spectroscopy for the investigation of the magnon BEC dynamics in a single-crystal film of yttrium iron garnet in a wide temperature range from 30 K to 380 K. By comparing the BLS results with previous microwave measurements, we revealed the direct relation between the damping of the condensed and the parametrically injected magnons. The enhanced supercurrent dynamics was detected at 180 K near the minimum of BEC damping.

K e y w o r d s: magnon gas, parametric pumping, Bose–Einstein condensate, magnon superfluidity, magnon supercurrent, yttrium iron garnet (YIG).

1. Introduction

The phenomena related to room-temperature Bose–Einstein condensation [1–6] and superfluidity [7–9] in overpopulated magnon gases constitute a fastly evolving field of research, revealing promising features for advanced technological applications [10] and discovery of novel physical effects [11–16]. Recent examples of such phenomena are magnon supercurrents [7], Bogoliubov [9] and second sound [16] waves, microscaled vorticity [8] in a magnon condensate, thermally induced magnon Bose–Einstein Condensates (BECs) in microsized magnetic structures [17,18], and the interaction of the magnon BEC with accumulated hybrid magnetoelastic bosons [19]. The intrinsic coherence of magnon BECs, allowing for a phase-encoded information processing and a long-range supercurrent-carried data transfer in the GHz regime, creates the potential for applications of these macroscopic quantum phenomena in the field of wave-based computing.

Here, we investigate the process of Bose–Einstein condensation of parametrically pumped magnons in a single-crystal Yttrium Iron Garnet [20] (YIG, $Y_3Fe_5O_{12}$) film in a wide range of temperatures (from 380 K down to 30 K). The temperature dependence of the magnon BEC decay rate is in quantitative agreement with the temperature dependence of the relaxation rates of the parametrically injected magnons [21]. In particular, both relaxation rates exhibit a non-monotonous behavior, with a minimum at around 200 K and a large increase for temperatures

below 100 K. The magnon supercurrents, which manifest themselves in our experiments in the enhanced magnon BEC decay, were found to be most prominent around 180 K, i.e., in the regime where the magnon damping is minimal.

2. Experimental Setup

To investigate the temperature dependence of the magnon condensate properties, we designed a setup composed of a microwave circuit for the parametric excitation of magnons and a Brillouin Light Scattering (BLS) spectroscopy part for magnon detec-
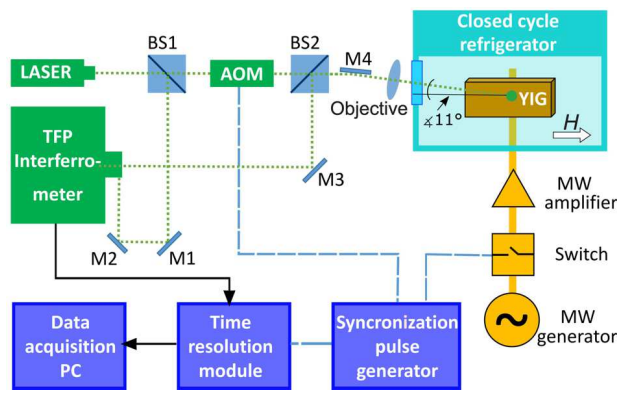
Fig. 1. Sketch of the experimental setup composed of a Brillouin light scattering spectroscopy part (green), microwave excitation circuit (yellow), temperature control part (cyan), and time synchronization and data acquisition part (blue). M1-M4 – mirrors. BS1 – beam splitter. BS2 – polarizing beam splitter. H – bias magnetic field
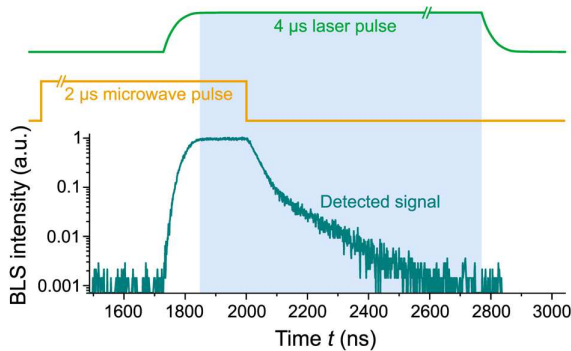
Fig. 2. Schematics of the relevant time intervals. Top: the 2 μs long MW pumping pulse (yellow) and the 4 μs long pulsed BLS laser beam (green). Bottom: the plot of the resulting detected BLS photon counts (magnon density) over time, detected at 180 K. The shaded area shows the part of the recorded data traces used for the analysis

tion [22] (see Fig. 1). The YIG sample is placed on top of a microstrip resonator, attached from below to a highly heat-conducting AlN substrate. This part of the setup is mounted inside of a Janis Research 10 K closed cycle refrigerator system with optical access.

For the parametric pumping process, a microwave (MW) pumping pulse of 2 μs duration at a frequency $\omega_{\mathrm{p}} = 2\pi \times 15$ GHz with an 1 ms repetition rate and a maximal pumping power P_{p} of 12 W was applied to a microwave transmission line capacitively coupled to a 50 μm-wide microstrip resonator. The microwave Oersted field $\mathbf{h}_{\mathrm{p}}$ induced by the microstrip resonator parametrically drives the magnetization of the YIG-film sample [23]. The parametric pumping process [24, 25] can be understood as a decay of a microwave photon with frequency ω_{p} and nearly zero wavevector into two magnons at half the photon frequency $\omega_{\mathrm{p}}/2 = 2\pi \times 7.5$ GHz having opposite wavevectors $\mathbf{q}$ and $-\mathbf{q}$.

After the thermalization [26–28] of the parametrically injected magnons over the spin-wave spectrum, a quasiequilibrium distribution of the magnon gas is established. The effective chemical potential of such a quasiparticle system is nonzero and depends on the density of injected excessive magnons. At a sufficiently large pumping power, the chemical potential reaches the bottom of the magnon spectrum, and the Bose–Einstein condensation of magnons takes place [2, 3, 29, 30].

The time-resolved BLS spectroscopy measurements were performed in a backward scattering geometry [31]. In such a geometry, the incidence angle of the probing laser beam can be adjusted to selectively detect magnons with a particular value of the in-plane wavevector [32]. In the experimental data shown below, the incidence angle was fixed at 11°, which corresponds to the detection of magnons at the bottom of the spin-wave spectrum, where thermalized magnons accumulate and the magnon BEC is formed.

In order to reduce the optical heating of the YIG sample, the probing laser beam was chopped by an Acousto-Optic Modulator (AOM) into a sequence of light pulses of 4 μs duration (see Fig. 1). In the time-resolved experiments, the probing laser pulse has been applied 1.8 μs after the start of the microwave pumping pulse. This scheme allowed us to map the time evolution of the magnon BEC during both the pumping and free-decay stages (see Fig. 2).

The YIG sample used in the experiments has lateral dimensions of 1×5 mm^2 and a thickness of 5.6 μm. It was prepared by the chemical etching of an YIG film epitaxially grown in the (111) crystallographic plane on a GGG substrate 500 μm in thickness. The sample was magnetized along its long axis (see Fig. 1) to avoid the undesirable influence of a static demagnetizing field on the value of the internal magnetic field.

To achieve the most efficient condensation of magnons, we pumped the magnon gas at an applied magnetic field H corresponding to the kinetic instability regime [33–35]. Since the YIG saturation magnetization M_S is temperature-dependent, the external field was adjusted at each temperature to maximize the BLS signal [21]. Thus, the measurements have been performed at fields ranging from 1140 Oe to 1250 Oe.

The temporal profiles of the BEC intensity, measured in the temperature range 30–380 K, are shown in Fig. 3. To facilitate a comparison of the magnon decay processes at different temperatures, the BEC profiles have been normalized to their maximum intensity measured during the action of the microwave pumping pulse (the plateau region). In this work, we are mostly interested in the free decay of the magnon BEC, i.e. in the part of the temporal profiles measured after the pumping pulse was switched off (t =2000 ns in Fig. 3). Below, we show that the time dependences of the magnon intensity decay provide valuable information about the dissipation and the coherence properties of the magnon BEC.

3. Results

The temporal evolution of the BLS intensities, measured at different temperatures, is shown in Fig. 3. The observed relaxation dynamics is determined by a competition between several different processes. The first one is the conventional exponential magnon decay to the phonon bath. This linear process is dominant for small BEC densities at long observation times. At relatively high temperatures $T \gtrsim 200$ K (see Fig. 3, *a, b*), the rate of linear BEC decay increases with the temperature. At low temperatures $T \lesssim 200$ K, however, the trend changes, and the magnon BEC decay rate starts to increase as the temperature goes down (see Fig. 3, *c*). Thus, the rate of decay of the magnon BEC exhibits a clear minimum
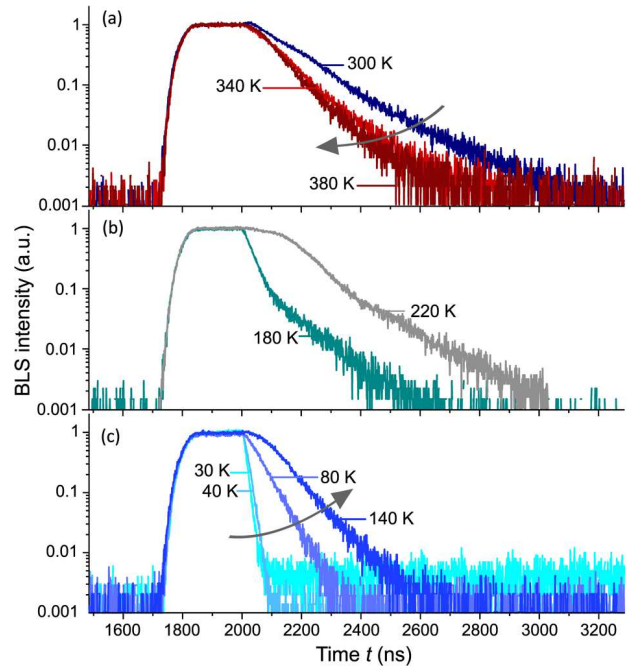
Fig. 3. Time profiles of the BLS intensity for different temperatures: 380 K to 300 K (*a*), 220 K and 180 K (*b*), and 140 K to 30 K (*c*). In panels (*a*) and (*c*), the temperature increases in the direction of the gray arrows. The decay characteristics of the profiles at $t > 2100$ ns provide information about the dissipation and redistribution of the magnon BEC

at temperatures around $T \approx 200$ K. The increase of the decay rate at higher temperatures $T > 200$ K can be explained by the scattering of condensed coherent magnons on higher-energy thermally excited incoherent magnons. The increase of the damping at low temperatures is, most probably, related to the magnon absorption in the paramagnetic GGG substrate and to their scattering at magnetic impurities in a YIG film [21, 36–38].

At short times after the pumping pulse is switched off, the BEC dynamics cannot be described by a simple exponential decay function [39]. First of all, here, the BEC density is influenced by the thermalization of parametrically injected magnons, which continues for some time after the pumping is switched off [3, 29, 30]. This process results in the cascade transition of the thermalized magnons previously scattered over higher energy states to the magnon BEC and, thus, decelerates the natural exponential decay of the condensed magnon phase. Such an effect is especially visible for the temperatures of 140 K and 220 K.
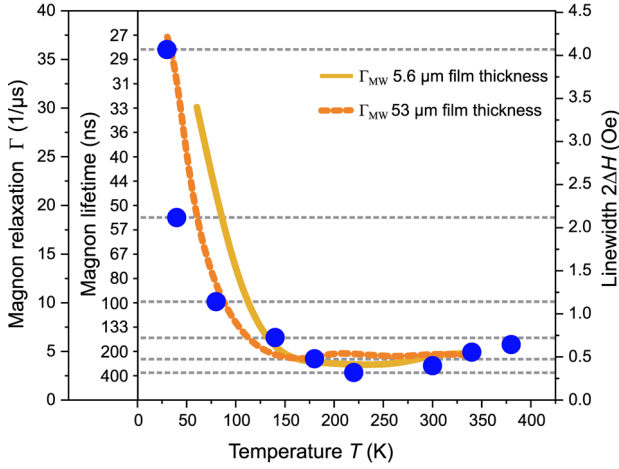
Fig. 4. Temperature dependence of the magnon relaxation parameter Γ, lifetime $\tau = 1/\Gamma$ (left axes), and the damping related linewidth $2\Delta H = 2\Gamma/\gamma$ (right axis). Here, $\gamma = 2\pi \times \times 2.8$ MHz/Oe is the modulus of the gyromagnetic ratio. Points – damping of the magnon BEC measured in this work; lines – damping of parametrically injected magnons in YIG films of two different thicknesses (from Ref. [21])

At the same time, there is another process, which accelerates the decrease in the BEC density. Its influence is most clearly visible for $T = 180$ K (see Fig. 3, *b*). The initial fast decrease in the BLS intensity is not related to any dissipation mechanism, but is a signature of magnon supercurrents [7, 9, 35], which lead to a spatial redistribution of the coherent magnon BEC [9]. This coherent redistribution process–outflow of the magnon BEC from the hot laser spot–is driven by a thermally induced phase gradient within the BEC wavefunction [7, 9, 35].

This coherent phenomenon strongly depends on the BEC density and, thus, on its lifetime. In our experiment, the supercurrent-related decay is the most pronounced at temperatures of 180 K and 220 K, where the natural magnon relaxation rate is near its minimal value, and becomes much less pronounced with a decrease in the magnon lifetime.

In the following analysis, we neglect the initial part of the decaying magnon BEC intensity profile $I(t)$, in which post-pumping thermalization processes and magnon supercurrents are important, and fit the remaining part with the exponential function

$$I(t) \sim e^{-2\Gamma t}, \qquad (1)$$

where the fitting parameter Γ has the meaning of a magnon BEC relaxation rate (i.e., the relaxation rate

of magnons at the bottom of the magnon spectrum) [24]. The results of this analysis are shown in Fig. 4, together with the temperature dependence of the rate of relaxation of parametrically injected magnons measured in Ref. [21]. Here, the dimensionless data from Ref. [21] were scaled to coincide with the BEC relaxation rate at one temperature point $T = 340$ K.

As is clearly seen from Fig. 4, the relaxation rates for both groups of magnons have the same qualitative and quantitative temperature dependence. The magnon damping is minimal around $T \approx 200$ K, slowly increases for higher temperatures, and demonstrates a large increase for $T < 150$ K. At the same time, this low-temperature relaxation increase is visibly slower for the magnon BEC, than for the parametric magnons excited in the same YIG film (solid yellow curve in Fig. 4). The behavior of the BEC relaxation rate is much closer to the temperature dependence of parametric magnons measured in the 10 times thicker YIG film of 53 μm thickness (dashed orange curve in Fig. 4). One possible explanation of this fact might be a slightly weaker coupling of the condensed short-wavelength dipole-exchange magnons (BEC wavenumbers $q_{BEC} \approx \pm 4 \times \times 10^4$ rad cm^{-1}) [3] to the paramagnetic spin structure of the GGG substrate in comparison with such a coupling of the rather long-wavelength dipolar magnons ($q \to 0$) parametrically excited and characterized in work [21]. This coupling is expected to be smaller in a thicker film, than in a thinner one, and, thus, the BEC relaxation rates in the thinner film come closer to the relaxation of long-wavelength parametric magnons in the thicker one.

4. Conclusions

We have experimentally measured the temperature dependence of the rate of relaxation of magnons at the bottom of the magnon spectrum (at the point of magnon Bose–Einstein condensation). We have found that the temperature dependence of the damping of magnons in this spectral range is in a quantitative agreement with the damping of another important group of short-wavelength magnons – those, which are directly injected by microwave parametric pumping. Namely, the magnon damping has a minimum at $T \approx 200$ K and increases for both higher and lower temperatures. We have also found that magnon BEC supercurrents are strongly enhanced in the temperature range near the magnon damping minimum. The

similar temperature behavior of the magnon BEC and parametrically injected magnons brings hope for that an extremely long BEC lifetime can be achieved in ultra pure bulk YIG samples, where, as it has been found in Refs. [21, 40], the rate of relaxation of parametric magnons monotonically decreases from room to cryogenic temperatures.

1. G.A. Melkov, V.L. Safonov, A.Y. Taranenko, S.V. Sholom. Kinetic instability and Bose condensation of nonequilibrium magnons. *J. Magn. Magn. Mater.* **132**, 180 (1994).

2. S.O. Demokritov, V.E. Demidov, O. Dzyapko, G.A. Melkov, A.A. Serga, B. Hillebrands, A.N. Slavin. Bose–Einstein condensation of quasi-equilibrium magnons at room temperature under pumping. *Nature.* **443**, 430 (2006).

3. A.A. Serga, V.S. Tiberkevich, C.W. Sandweg, V.I. Vasyuchka, D.A. Bozhko, A.V. Chumak, T. Neumann, B. Obry, G.A. Melkov, A.N. Slavin, B. Hillebrands. Bose–Einstein condensation in an ultra-hot gas of pumped magnons. *Nat. Commun.* **5**, 3452 (2014).

4. A.I. Bugrij, V.M. Loktev. On the theory of Bose–Einstein condensation of quasiparticles: On the possibility of condensation of ferromagnons at high temperatures. *Low Temp. Phys.* **33**, 37 (2007).

5. S.M. Rezende. Theory of coherence in Bose–Einstein condensation phenomena in a microwave-driven interacting magnon gas. *Phys. Rev. B* **79**, 174411 (2009).

6. Y.M. Bunkov, V.L. Safonov. Magnon condensation and spin superfluidity. *J. Magn. Magn. Mater.* **452**, 30 (2018).

7. D.A. Bozhko, A.A. Serga, P. Clausen, V.I. Vasyuchka, F. Heussner, G.A. Melkov, A. Pomyalov, V.S. L'vov, B. Hillebrands. Supercurrent in a room-temperature Bose–Einstein magnon condensate. *Nat. Phys.* **12**, 1057 (2016).

8. P. Nowik-Boltyk, O. Dzyapko, V.E. Demidov, N.G. Berloff, S.O. Demokritov. Spatially non-uniform ground state and quantized vortices in a two-component Bose–Einstein condensate of magnons. *Sci. Rep.* **2**, 482 (2012).

9. D.A. Bozhko, A.J.E. Kreil, H.Yu. Musiienko-Shmarova, A.A. Serga, A. Pomyalov, V.S. L'vov, B. Hillebrands. Bogoliubov waves and distant transport of magnon condensate at room temperature. *Nat. Commun.* **10**, 2460 (2019).

10. A.V. Chumak, V.I. Vasyuchka, A.A. Serga, B. Hillebrands. Magnon spintronics. *Nat. Phys.* **11**, 453 (2015).

11. K. Nakata, K.A. van Hoogdalem, P. Simon, D. Loss. Josephson and persistent spin currents in Bose–Einstein condensates of magnons. *Phys. Rev. B* **90**, 144419 (2014).

12. K. Nakata, P. Simon, D. Loss. Magnon transport through microwave pumping. *Phys. Rev. B* **92**, 014422 (2015). http://dx.doi.org/10.1103/PhysRevB.92.014422

13. H. Skarsvåg, C. Holmqvist, A. Brataas. Spin superfluidity and long-range transport in thin-film ferromagnets. *Phys. Rev. Lett.* **115**, 237201 (2015).

14. V.I. Sugakov. Formation of new phase inclusions in the system of quasiequilibrium magnons of high density. *Phys. Rev. B* **94**, 014407 (2016).

15. B. Flebus, S.A. Bender, Y. Tserkovnyak, R.A. Duine. Two-fluid theory for spin superfluidity in magnetic insulators. *Phys. Rev. Lett.* **116**, 117201 (2016).

16. V. Tiberkevich, I.V. Borisenko, P. Nowik-Boltyk, V.E. Demidov, A.B. Rinkevich, S.O. Demokritov, A.N. Slavin. Excitation of coherent second sound waves in a dense magnon gas. *Sci. Rep.* **9**, 9063 (2019).

17. C. Safranski, I. Barsukov, H.K. Lee, T. Schneider, A.A. Jara, A. Smith, H. Chang, K. Lenz, J. Lindner, Y. Tserkovnyak, M. Wu, I.N. Krivorotov. Spin caloritronic nano-oscillator. *Nat. Commun.* **8**, 117 (2017).

18. M. Schneider, T. Brächer, V. Lauer, P. Pirro, D.A. Bozhko, A.A. Serga, H.Yu. Musiienko-Shmarova, B. Heinz, Q. Wang, T. Meyer, F. Heussner, S. Keller, E.Th. Papaioannou, B. Lägel, T. Löber, V.S. Tiberkevich, A.N. Slavin, C. Dubs, B. Hillebrands, A.V. Chumak. Bose–Einstein condensation of quasi-particles by rapid cooling. arXiv:1612.07305v2 (2018).

19. D.A. Bozhko, P. Clausen, G.A. Melkov, V.S. L'vov, A. Pomyalov, V.I. Vasyuchka, A.V. Chumak, B. Hillebrands, A.A. Serga. Bottleneck accumulation of hybrid magnetoelastic bosons. *Phys. Rev. Lett.* **118**, 237201 (2017).

20. V. Cherepanov, I. Kolokolov, V. L'vov. The saga of YIG: Spectra, thermodynamics, interaction and relaxation of magnons in a complex magnet. *Phys. Rep. – Rev. Sec. Phys. Lett.* **229**, 81 (1993).

21. L. Mihalceanu, V.I. Vasyuchka, D.A. Bozhko, T. Langner, A.Yu. Nechiporuk, V.F. Romanyuk, B. Hillebrands, A.A. Serga. Temperature-dependent relaxation of dipole-exchange magnons in yttrium iron garnet films. *Phys. Rev. B* **97**, 214405 (2018).

22. A.A. Serga, C.W. Sandweg, V.I. Vasyuchka, M.B. Jungfleisch, B. Hillebrands, A. Kreisel, P. Kopietz, M.P. Kostylev. Brillouin light scattering spectroscopy of parametrically excited dipole-exchange magnons. *Phys. Rev. B* **86**, 134403 (2012).

23. T. Neumann, A.A. Serga, V.I. Vasyuchka, B. Hillebrands. Field-induced transition from parallel to perpendicular parametric pumping for a microstrip transducer. *Appl. Phys. Lett.* **94**, 192502 (2009).

24. A.G. Gurevich, G.A. Melkov, *Magnetization oscillations and waves* (CRC Press, 1996) [ISBN: 9780849394607].

25. G.A. Melkov, A.A. Serga, A.N. Slavin, V.S. Tiberkevich, A.N. Oleinik, A.V. Bagada. Parametric interaction of magnetostatic waves with a nonstationary local pump. *J. Exp. Theor. Phys.* **89**, 1189 (1999).

26. V. Demidov, O. Dzyapko, S. Demokritov, G. Melkov, A. Slavin. Thermalization of a parametrically driven magnon gas leading to Bose–Einstein condensation. *Phys. Rev. Lett.* **99**, 037205 (2007).

27. J. Hick, T. Kloss, P. Kopietz. Thermalization of magnons in yttrium-iron garnet: Nonequilibrium functional renormalization group approach. *Phys. Rev. B* **86**, 184417 (2012).

28. P. Clausen, D.A. Bozhko, V.I. Vasyuchka, B. Hillebrands, G.A. Melkov, A.A. Serga. Stimulated thermalization of a parametrically driven magnon gas as a prerequisite for Bose–Einstein magnon condensation. *Phys. Rev. B* **91**, 220402 (2015).

29. V.E. Demidov, O. Dzyapko, M. Buchmeier, T. Stockhoff, G. Schmitz, G.A. Melkov, S.O. Demokritov. Magnon kinetics and Bose–Einstein condensation studied in phase space. *Phys. Rev. Lett.* **101**, 257201 (2008).

30. D.A. Bozhko, P. Clausen, A.V. Chumak, Y.V. Kobljanskyj, B. Hillebrands, A.A. Serga. Formation of Bose–Einstein magnon condensate via dipolar and exchange thermalization channels. *Low Temp. Phys.* **41**, 801 (2015).

31. S.O. Demokritov, B. Hillebrands, A.N. Slavin. Brillouin light scattering studies of confined spin waves: linear and nonlinear confinement. Phys. Rep. **348**, 441 (2001).

32. C.W. Sandweg, M.B. Jungfleisch, V.I. Vasyuchka, A.A. Serga, P. Clausen, H. Schultheiss, B. Hillebrands, A. Kreisel, P. Kopietz. Wide-range wavevector selectivity of magnon gases in Brillouin light scattering spectroscopy. *Rev. Sci. Instrum.* **81**, 073902 (2010).

33. A.V. Lavrinenko, V.S. L'vov, G.A. Melkov, V.B. Cherepanov. "Kinetic" instability of a strongly nonequilibrium system of spin waves and tunable radiation of a ferrite. *Sov. Phys. JETP* **54**, 542 (1981).

34. G.A. Melkov, S.V. Sholom. Kinetic instability of spin waves in thin ferrite films. *Sov. Phys. JETP* **72**, 341 (1991).

35. A.J.E. Kreil, D.A. Bozhko, H.Yu. Musiienko-Shmarova, V.I. Vasyuchka, V.S. L'vov, A. Pomyalov, B. Hillebrands, A.A. Serga. From kinetic instability to Bose–Einstein condensation and magnon supercurrents. *Phys. Rev. Lett.* **121** 077203 (2018).

36. V.V. Danilov, D.L. Lyfar', Yu.V. Lyubon'ko, A.Yu. Nechiporuk, S.M. Ryabchenko. Low-temperature ferromagnetic resonance in epitaxial garnet films on paramagnetic substrates. *Sov. Phys. Journal* **32**, 276 (1989).

37. I. Boventer, M. Pfirrmann, J. Krause, Y. Schön, M. Kläui, M. Weides. Complex temperature dependence of coupling and dissipation of cavity magnon polaritons from millikelvin to room temperature. *Phys. Rev. B* **97**, 184420 (2018).

38. S. Kosen, A.F. van Loo, D.A. Bozhko, L. Mihalceanu, A.D. Karenowska. Microwave magnon damping in YIG films at millikelvin temperatures. arXiv: 1903.02527 (2019).

39. A.J.E. Kreil, H.Yu. Musiienko-Shmarova, D.A. Bozhko, S. Eggert, A.A. Serga, B. Hillebrands, A. Pomyalov, V.S. L'vov. Tunable space-time crystal in room-temperature magnetodielectrics. *Phys. Rev. B Rapid Commun.* (2019).

40. V.V. Danilov, A.Yu. Nechiporuk, L.V. Chevnyuk. Temperature dependences of paramagnetic excitation threshold and relaxation parameter of spin waves in garnet structures. *Low Temp. Phys.* **22**, 802 (1996).

Л. Міхалціну, Д.А. Божко,
В.І. Васючка, О.О. Серга, Б. Хіллебрандс,
А. Помялов, В.С. Львов, В.С. Тиберкевич

БОЗЕ–ЕЙНШТЕЙНІВСЬКИЙ КОНДЕНСАТ
МАГНОНІВ І СУПЕРСТРУМИ В ШИРОКОМУ
ІНТЕРВАЛІ ТЕМПЕРАТУР

Р е з ю м е

Магнонні бозе-ейнштейнівські конденсати (БЕК) та суперструми – це когерентні квантові явища, що виникають на макроскопічному масштабі в параметрично заселених спінових системах в твердих тілах. Одна з найбільш захоплюючих та привабливих рис цих процесів – можливість магнонної конденсації та збудження суперструмів навіть при кімнатній температурі. Водночас, цінна інформація про магнонні конденсати, така як час життя, поріг формування і ступінь когерентності, може бути отримана в експериментах, проведених при різних температурах. Ми використовуємо спектроскопію бріллюенівського розсіяння світла (БРС) для вивчення динаміки БЕК магнонів в монокристалічній плівці залізо-ітрієвого гранату в широкому інтервалі температур від 30 К до 380 К. Порівнюючи результати БРС з попередніми надвисокочастотними вимірами, ми виявили прямий зв'язок між затуханням конденсованих та параметрично інжектованих магнонів. Посилена динаміка суперструму зареєстрована при 180 К поблизу мінімуму затухання БЕК.